Supplementary information

Removal of pharmaceuticals and illicit drugs from wastewater due to ferric dosing in sewers

*Jagadeeshkumar Kulandaivelu[1], Jianfa Gao[2], Yarong Song[1], Sohan Shrestha[1], Xuan Li[1], Jiaying Li[1], Katrin Doederer[1], Jurg Keller[1], Zhiguo Yuan[1], Jochen F. Mueller[2], Guangming Jiang[1,3,4, *]*

This supplementary information contains the information such as rising main sewer reactor setup, properties of selected organic MPs, chemical spiking scheme in the cycle experiments conducted at the control and the ferric dosed sewer reactor, performance of analytical method for selected MPs, characteristics of particles formed in ferric dosed reactor, atomic ratio of iron and sulfide based on weight % obtained from EDS and ICP-OES, biodegradation of compounds in the control and ferric dosed reactor, comparison of biodegradation results with previous studies, simulated transformation coefficients of the investigated compounds with/without iron dosage, FTIR-ATR analysis depicting adsorption of MPs on the FeS particles, microbial community analysis & elemental composition of the biofilm and additional experiments to investigate the role of various iron particles formed by iron dosing.

Pages – S1 – S29

Tables – S1 – S8

Figures – S1 – S10

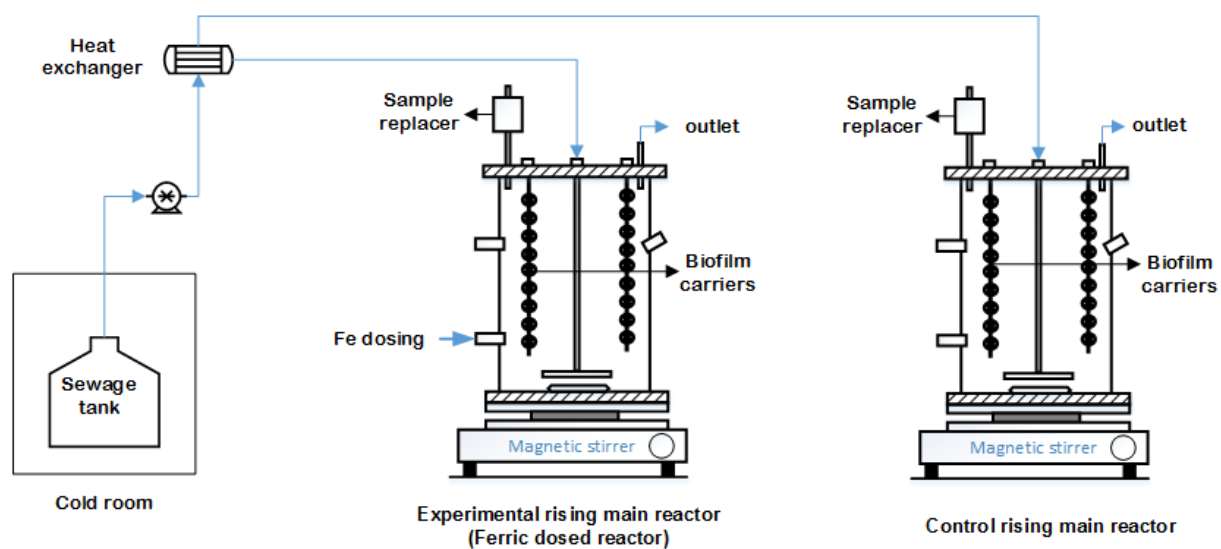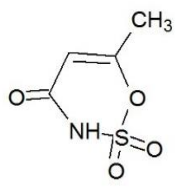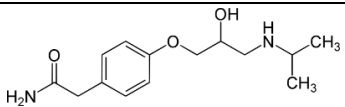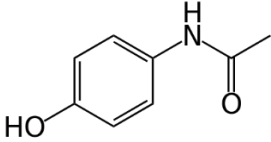# S1. RISING MAIN SEWER REACTOR SETUP
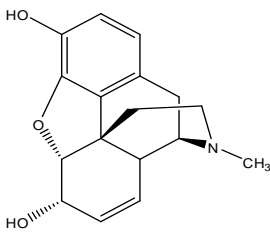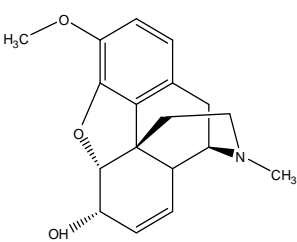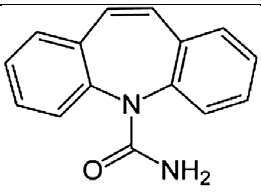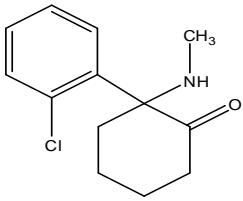
Figure S1. Schematic diagram of rising main sewer reactor setup

Table S1. Properties of selected organic MPs

Name	Structure	Log K_{ow}	pKa	MW (g/mol)
Acesulfame		-1.33	5.6	163.1
Atenolol		0.16	9.6	266.3
Paracetamol		0.46	9.8	151.2
Morphine		0.89	8.2	285.3
Codeine		1.19	8.2	299.4
Carbamazepine		2.45	13.9	236.3
Ketamine		3.12	7.4	237.7

Methadone		3.93	8.9	309.4

Table S2. Chemical spiking scheme in the cycle experiments conducted at the control and the ferric dosed sewer reactor (Section 2).

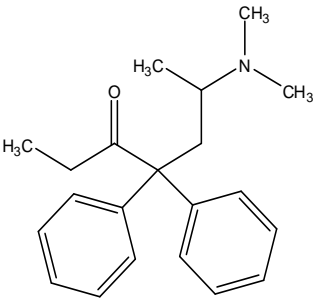| Cycle experiment in control and ferric dosed reactor					
Chemical	Spiked concentration (ppb)	Supplier Calibration std. / spike solution	Background concentration (ppb)	Average initial concentration obtained (ppb)	Recovery after spiking in the reactor (%)
Illicit drugs					
Ketamine	50	Cerilliant/Provet	0.33	48	94.7
Methadone	10	Cerilliant/Provet	0.12	13.6	133[*]
Morphine	20	Cerilliant/Provet	2.2	23.5	95.9
Codeine	10	Cerilliant/Provet	1.5	7.8	55[**]
Pharmaceuticals					
Carbamazepine	10	Local chemist shop	0.5	6	52.4[**]
Atenolol	20	Sigma Aldrich	1.2	26	117
Acesulfame	20	Sigma Aldrich	10.5	37	87

*the high recovery could be due to the inaccuracy of the human/vet drug injection solution used to prepare the spike solutions. **It is prepared by dissolving the tablet form.

Table S3. The performance of analytical method for selected MPs

Compound name	LOD	LOR	Relative error, %	Correlation coefficient
Codeine	0.03	0.10	9.27	0.999752
Morphine	0.03	0.10	7.29	0.999854
Methadone	0.02	0.05	4.03	0.999898
Ketamine	0.02	0.05	4.11	0.999466
Carbamazepine	0.02	0.05	1.31	0.999805
Paracetamol	0.05	0.10	4.72	0.997999
Atenolol	0.02	0.05	4.87	0.999855
Acesulfame	0.07	0.20	1.06	0.999873

Note: LOD (Limit of detection) was calculated as 3 time of standard deviation of 6 times injection of 0.1 µg/L standard. LOR (Limit of report) was calculated as 9 times of standard deviation of 6 times injection of 0.1 µg/L. Correlation coefficient is demonstrated by the r of the calibration curve.

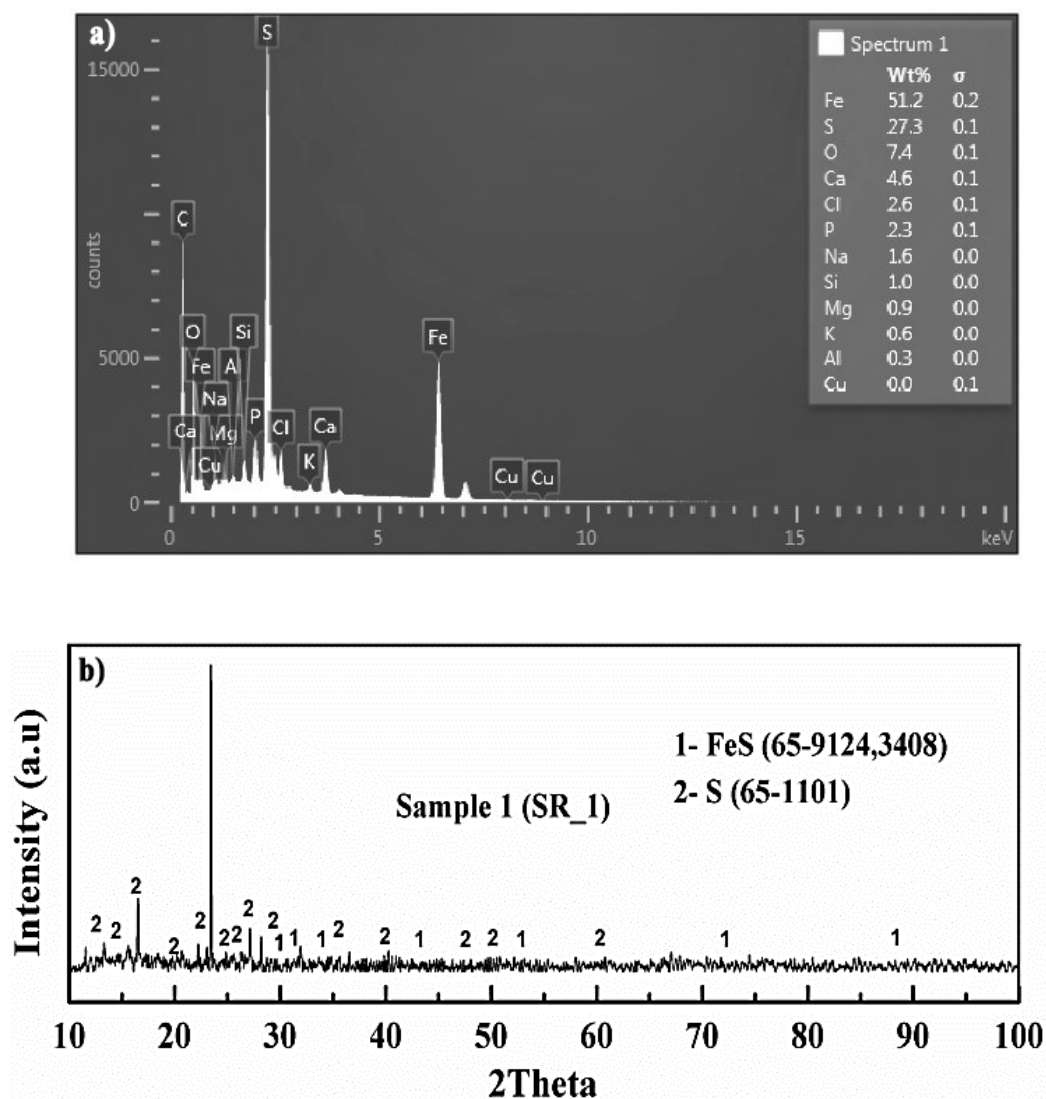## S2. CHARACTERIZATION OF PARTICLES FORMED IN IRON DOSED REACTOR

Figure S2. (a) Elemental composition (Wt %)of particles formed in the ferric dosed reactor by Energy Dispersive X-ray spectra (b) XRD pattern of the particles collected from the ferric dosed reactor
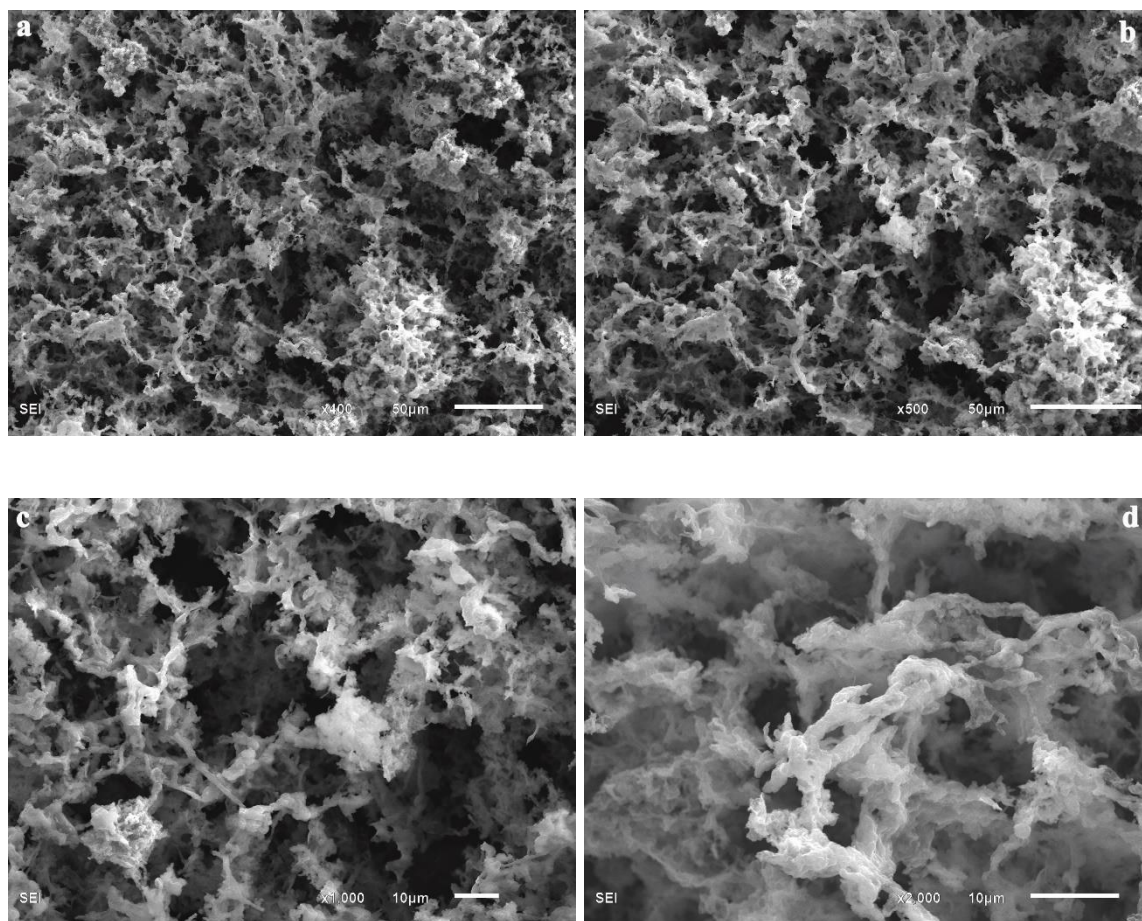
Figure S3. SEM images of suspended particles collected from ferric dosed sewer reactor, with different magnification a) x400 b) x500 c) x1000 d) x2000

Table S4. Atomic ratio of iron and sulfide based on the weight % obtained from EDS of four selected spots

Spots on the FeS particles	Weight (%)		Atomic (%)		Atomic ratio	Assumed Conc.
	Fe	S	Fe	S		
Spot-1	51.2	27.3	0.92	0.85	1.08	FeS
Spot-2	48.4	28.2	0.87	0.88	0.98	FeS
Spot-3	21.7	15.2	0.39	0.47	0.82	FeS
Spot-4	31.4	26.1	0.56	0.81	0.69	FeS_2

Table S5. Total Fe and S atomic ratio based on the elemental concentration measured by ICP-OES for wastewater samples from the ferric dosed sewer reactor

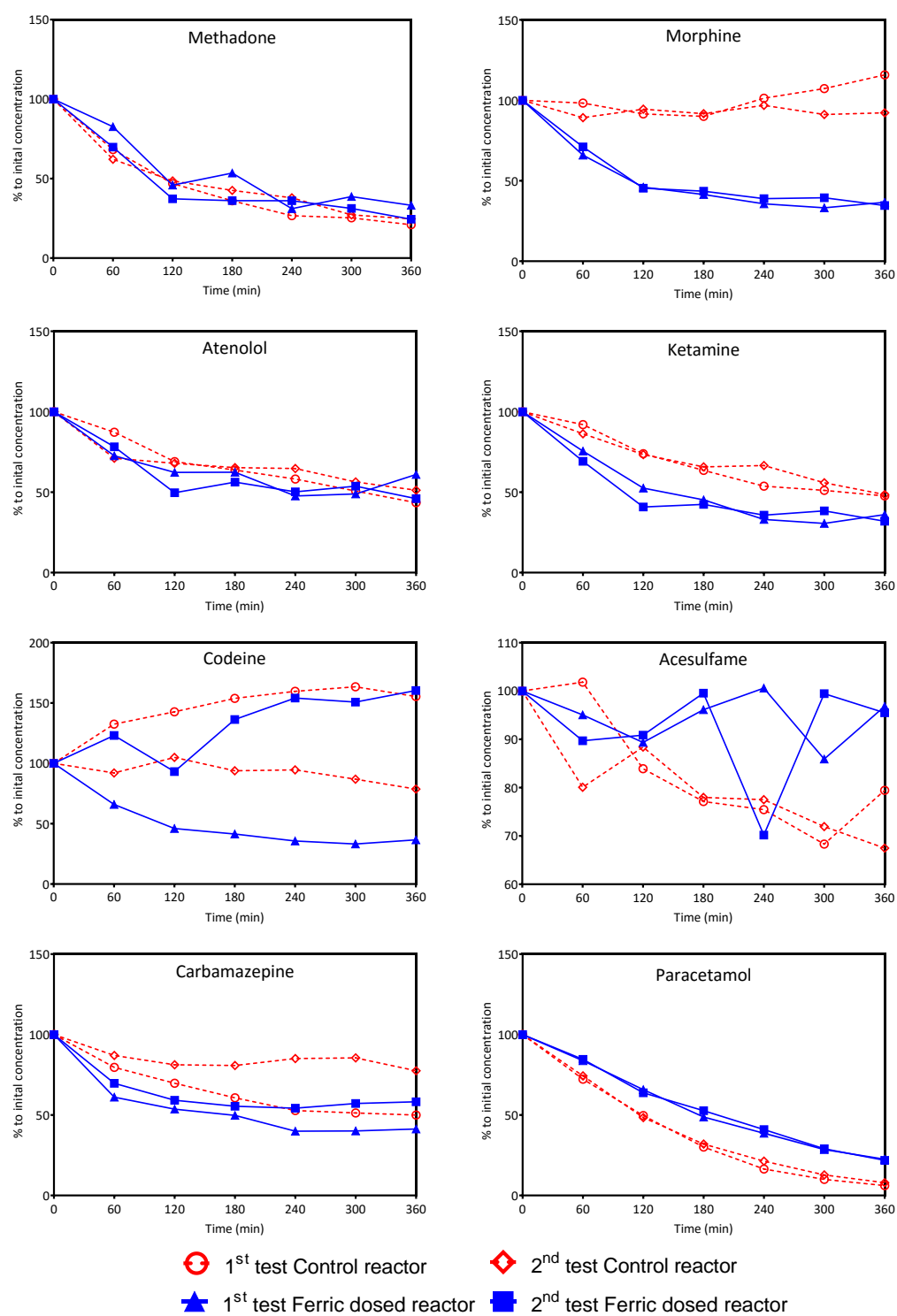| Time (h)	Average Total Fe (mg/L)	Average Total S (mg/L)	Molar ratio Fe : S
0.00	76.03	29.95	1.46
1.00	59.35	23.56	1.45
2.00	47.36	20.10	1.35
3.00	46.93	29.95	0.90
4.00	48.98	31.35	0.90
5.00	50.91	29.52	0.99
6.00	56.57	34.19	0.95

Figure S4. Biotransformation of selected MPs in the control and ferric dosed reactor. In the ferric dosed reactor, the concentration after five minute of spiking the compound was considered as the initial concentration

Table S6. Comparison of the degradation percentage of selected MPs with previous studies in literature.

Compound	Baker et al.[1]	Van Nuijs et al.[2]	Chen et al.[3]	Ostman et al.[4]	Senta et al.[5]	Ramin et al.[6]	McCall et al.[7]	Gao et al.[8]	This study Control reactor	This Study Experiment reactor
	Unfiltered WW, pH=7.4, 19 °C, 24h	Wastewater pH=7.5, 20 °C, 26h	Unfiltered Wastewater pH=7, 20°C, 24h	Unfiltered wastewater; room temperature; 24h	Unfiltered wastewater; 20 °C, pH=7.5	Unfiltered wastewater; pH=8-9; 15°C, 24h	Wastewater with suspended biofilm at A/V of 17-66 m²/m³; pH=7-9; 20 °C; 24h	Rising main sewer reactor, pH=7.5; 20 °C; 12h	Rising main reactor, pH=6.9, 6h, 20 °C	Rising main reactor, pH=6.85, 6h, 20 °C
Group - 1										
Methadone	<10%	<5%	<5%	<5%	<10%	>80%	>80%	76 ± 9%	77 ± 3 %	99 %
Morphine	-	-	-	-	-	-	-	-	-4 ± 17 %	97 %
Atenolol	NA	NA	NA	NA	NA	NA	NA	NA	53 ± 5.5 %	93 ± 0.8 %
Group-2										
Ketamine	<10%	NA	NA	<10%	NA	NA	Up to 30%	56 ± 17%	52 %	91%

Codeine	<15%	NA	<5%	<10%	<10%	NA	<20%	84 ± 8%	-17 ± 54 %	66 ± 14 %
Carbamazepine	NA	NA	NA	NA	NA	NA	NA	NA	36 ± 19 %	70 ± 3.50%
Acesulfame	NA	NA	NA	NA	NA	NA	NA	NA	26.5 ± 8.5%	35 ± 1 %
Group-3										
Paracetamol	NA	NA	NA	NA	NA	NA	NA	NA	93.12 ± 1.31 %	78.36 ± 0.23%

The numbers present in the table are the loss of selected compounds during the experiments

Table S7. Simulated transformation coefficients (mean (5% credible interval)) of the investigated compounds in sewers with/without iron dosage

Compounds	Control reactor	Ferric dosed reactor
Acesulfame	0.0605 (0.0415, 0.0799)	0.0033 (0, 0.0209)
Atenolol	0.1260 (0.1026, 0.1496)	0.1224 (0.0654, 0.1792)
Carbamazepine	0.0743 (0.0209, 0.1204)	0.1302 (0.0595, 0.2010)
Codeine	0.0022 (0, 0.0199)	0.0142 (0, 0.0941)
Ketamine	0.1290 (0.1145, 0.1440)	0.2351 (0.1752, 0.3005)
Methadone	0.2963 (0.2548, 0.3418)	0.2548 (0.1804, 0.3373)
Morphine	0.0012 (0, 0.0088)	0.2212 (0.1571, 0.2907)
Paracetamol	0.4032 (0.3771, 0.4293)	0.2456 (0.2310, 0.2605)

S.3. FTIR-ATR ANALYSIS DEPICTING ADSORPTION OF MPS ON THE FES PARTICLES

S.3.1 METHOD. The iron sulfides (FeS) were freshly prepared by spiking the iron (10 mg-Fe/L) and sulfide (20 mg-S/L) solutions to the filtered wastewater in a separate anaerobic reactor without biofilm. Then the FeS was taken and mixed with MPs in a 100mL serum bottle and were shaken at 200 rpm for one hour. Right before the FTIR analysis, the samples were centrifuged at 1500 rpm for 2 min without any air bubbles to prevent the any structural changes. The particles were then applied on the diamond ATR crystal and the ATR-FTIR spectra were recorded immediately. The ATR-FTIR spectra of FeS particles before and after mixing with MPs is shown in Figure S5.

S.3.2. RESULTS. FTIR spectra show that unreacted FeS sample comprises of different functional groups. As depicted in Figure S5, OH-stretching bonds were detected in IR spectrum of unreacted FeS sample as a broad peak in the region from 3000 to 3700 cm^{-1} [9]. The 3351.92 and 3236.08 cm^{-1} peaks are indicative of stretching of both normal 'polymeric' –OH and aliphatic primary amine –NH functional groups. Notably, aromatic C-H stretching also usually occurs above 3000 cm^{-1} wherein saturated C-H stretching absorptions all occur below 3000 cm^{-1}. The peaks 1998.934, 2054.241, 2090.656, 2111.382, 2172.894 and 2193.93 cm^{-1} observed in the range 1990 – 2285 cm^{-1} are associated with cyanates group or –O-C≡N stretching. Similarly, peaks observed in the range between 2100 and 2260 cm^{-1} are associated to alkyne compounds with peculiar C≡C bond stretching. The 1460.009 cm^{-1} band can be either asymmetric/symmetric bending vibrations of methyl C-H or methylene C-H groups. The band at 1630.184 cm^{-1} is due to either alkenyl C=C stretching or secondary amine N-H bending; it might be even hetero-oxy compounds (organic nitrates in this case). Also, IR spectra at 1630.184, 1550.375 and 1408.146 cm^{-1} is also resultant of C=O stretching, primarily associated

with carboxylate, amide or ketone. Aromatic nitro compounds or N=O vibrations is associated with peak at 1535.234 cm^{-1}. *Akin* the bands at 594.978, 500.018 cm^{-1} are associated with functionality of C-X stretching, where X is fluoro (F) – or iodo (I) – compounds herein. The band at 1028.9 cm^{-1} can be associated with different functionalities of either cyclohexane ring vibrations or stretching of C-F; it might also be primary amine C-N functional groups or aliphatic phosphates (P–O–C stretching). Further, 1258.919 cm^{-1} is associated with aromatic primary amine, C-N stretching. The bands 416.395, 428.361, 437.715, 447.389 and 481.106 cm^{-1} are corroborated due to S-S stretching (i.e., aryl disulfides or polysulfides)[10]. The IR spectra of similar characteristic peaks owing to different functional groups were also observed in FeS sample treated with different MPs *akin* to unreacted FeS sample (Figure S5). Additionally, characteristic peaks associated with Fe-S stretching and bending at low frequencies (< 450 cm^{-1}) were observed in both unreacted FeS and micropollutant reacted FeS [11].

Major characteristic peaks were somewhat similar in IR spectra of both samples (Figure S5), whilst relatively both samples depicted some noticeable shifts or changes in some of the characteristics absorbance bands. Table S8 depicts the major differences between the intensity of peaks in both samples. Majority of peaks intensity associated with different functionality (i.e., wavenumber changes) in unreacted FeS samples were higher than in FeS sample treated with different MPs. However, few peaks intensity were comparatively lower in unreacted FeS sample. Notably, some of the characteristics peaks observed in unreacted FeS sample were not observed in treated FeS sample. This result vividly indicates adsorption of MPs on FeS surface as the main mechanism behind the removal of MPs on treating with FeS particles under anaerobic sewer condition. Further, disappearance or increment in some of the characteristics

peaks in treated FeS sample suggest that this adsorption process could be taking place via both ion-exchange and complexation pathways [12, 13].

Table S8. Major FTIR spectra changes of FeS sample after treatment with different MPs

FeS [Wavenumbers, cm⁻¹]	FeS with MPs (60 min) [Wavenumbers, cm⁻¹]	Change/shift in wavenumbers (ΔWavenumbers, cm⁻¹)
3857.685	3631.866	225.819
3842.202	3652.491	189.711
3351.92	3359.68	-7.76
3236.08	3247.715	-11.635
2659.622		-
2287.788		-
2193.93	2215.025	-21.095
2172.894	2140.984	31.91
2111.382	2117.003	-5.621
2090.656		-
2054.241	2061.533	-7.292
1950.795		-
1998.934		-
1630.184		-
1550.375	1550.384	-0.009
1535.234	1534.419	0.815
1460.009		-
1408.146		-
1258.919	1260.405	-1.486
1028.59	1027.167	1.423
594.978		-

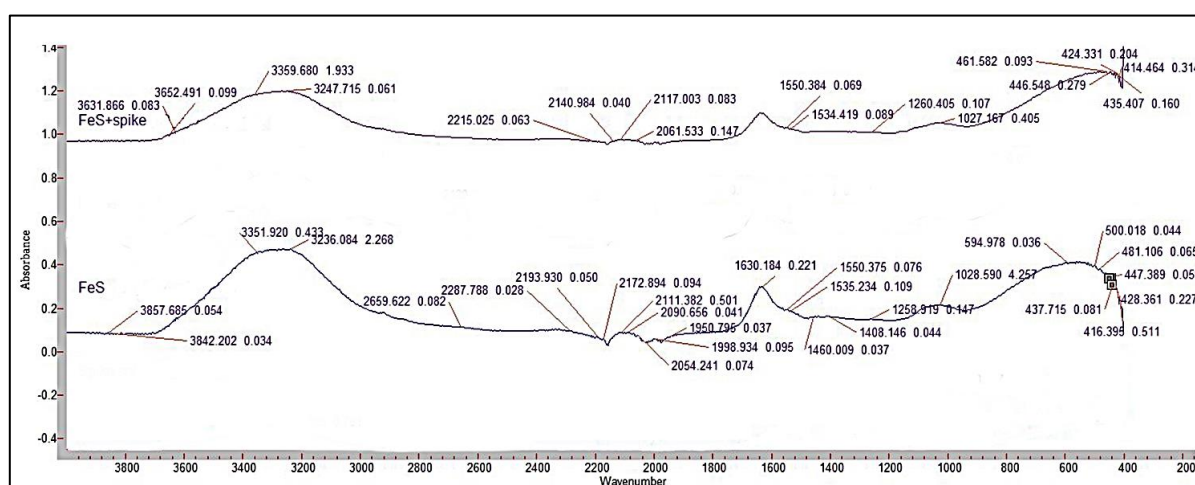|		
500.018		-
481.106	461.582	19.524
447.389	446.548	0.841
428.361	424.331	4.03
437.715	435.407	2.308
416.395	414.464	1.931

Figure S5. FTIR spectra of both unreacted and MPs treated FeS samples

S.4. BIOFILM CHARACTERISATION

S.4.1. MATERIALS AND METHODS

S.4.1.1. MICROBIAL COMMUNITY ANALYSIS (MCA). To identify the microbial community of the sewer biofilms and the effect of ferric dosing on the microbial community, MCA was carried out in both control and the ferric dosed reactor. For DNA extraction, the biofilms on the walls of the reactor were scrapped with a sterile surgical scalpel into a 2 mL Eppendorf vials. The DNA of the biofilms were extracted right after collection using the Fast DNA^{TM} SPIN Kit for Soil (MP Biomedicals, CA, USA), as per manufacture's instruction. To perform 16S rRNA gene amplicon sequencing (Illumina), extracted DNA samples were provided to the Australia Center for Ecogenomics (ACE, Brisbane, Australia). The extracted 16S rRNA gene was amplified using the universal primer set 926F (5'-AAACTYAAAKGAATTGACGG-3') and 1392R (5'-ACGGGCGGTGTGTRC-3'). The resulting PCR amplicons were purified using Agencourt AMPure XP beads (Beckman Coulter). Then the purified DNA was indexed using the Illumina Nextera XT 384 sample Index Kit A-D (Illumina FC-131-1002) in standard PCR conditions with Q5 Hot Start High-Fidelity2X Master Mix. The indexed amplicons were pooled together in equimolar concentrations and sequenced on MiSeq Sequencing System (Illumina) at ACE according to manufacturer's protocol.

Raw sequencing data were quality-filtered and demultiplexed using Trimmomatic, with poor-quality sequences trimmed and removed. Subsequently, high-quality sequences at 97% similarity were clustered into operational taxonomic units (OTUs) using QIIME (an open source for bioinformatics database) with default parameters, and representative OTU sequences were taxonomically BLASTed against the Green genes 16S rRNA database. Finally, an OTU table consisting of the taxonomic classification and OTU representative sequences

were produced. The heat map was generated by average-linkage agglomeration method using R (version 3.31)[14].

S.4.1.2. ELEMENTAL COMPOSITION OF THE BIOFILM. To investigate the elemental composition, the biofilm was scratched from the sides of the ferric dosed reactor as mentioned in the previous section and were dried overnight in a vacuum oven (SEMSA OVEN 718). These particles were then tested for its properties using scanning electron microscopy-Energy dispersive X-ray spectrometry (SEM-EDS). The vacuum dried samples were carbon coated and measured using SEM (JEOL JSM-6610, America) equipped with a detector (Oxford 50 mm^2 X-Max SDD x-ray) as mentioned in section 2.7.

S.4.2. RESULTS

S.4.2.1. MCA. The microbial community present in the control and ferric dosed sewer reactor was shown in the Figure S6. *Caldisericum, Methanosaeta, Methanomassiliicoccus, Methanospirillum, Methanobacterium, Smithella, Romboutsia, Christensenellaceae R-7 group, Desulfurivibrio* were determined as the top 9 abundant microbes in both the reactors. Most of these microbes are functional microbes that have been commonly detected in sewer systems and can be divided into groups based on their functions. *Methanosaeta, Methanomassiliicoccus* belonging to the family *Methylophilaceae, Methanospirillum,* and *Methanobacterium* are the methanogenic archaea (MA) that are related to the methane production [15, 16]. Some microorganisms belonging to pseudomonas family are also present in the biofilm obtained from the control reactor (data not shown). The microorganisms belonging to the family *Methylphilaceae* and the pseudomonas were capable of degrading artificial sweetener such as acesulfame in the wastewater treatment plant [17]. *Smithella* are syntrophic propionate-oxidizing anaerobes under methanogenic, mesophilic temperature conditions [15]. *Caldisericum* was found as abundant microbes in active sludge treatment reactors and known

to have the capability for thiosulfate reducing [18, 19]. The genus *Romboutsia* was newly established in 2014 and shown to contribute in hydrogen production under anaerobic conditions [20]. *Christensenellaceae R-7 group* are anaerobic bacteria that can be found in the ruminal mucosa of goats and food waste digester [21, 22]. *Desulfovibrio* is a typical sulfate-reducing bacteria (SRB) that produces sulfide in the anaerobic parts of sewer facilities [23, 24]. This study mainly focuses on the SRB's and MA community. As some of the SRB's and MA's were not shown in the top abundant species, the abundance of SRB and MA throughout the whole samples were summarized in (Figure S7). The relative abundance of SRB in both the control and the ferric dosed reactor were 1.4 ±0.1% and 1.6±0.4% respectively. But, the relative abundance of MA in the ferric dosed reactor showed the relative decrease of 33.9±3.4% compared to the control sewer reactor. These results shows that the sulfate reduction was not impacted due to ferric dosing whereas the methane production was impacted in the ferric dosed reactor. These results are in agreement with the results obtained and discussed in section 3.1. Similar reduction in the abundance of MA and the reduction in the methane production was observed recently in the rising main sewers[25]. The microbial community of the sewer biofilms could vary based on quality of wastewater and the environmental conditions such as pH, oxidation-reduction potential and dissolved oxygen[26].
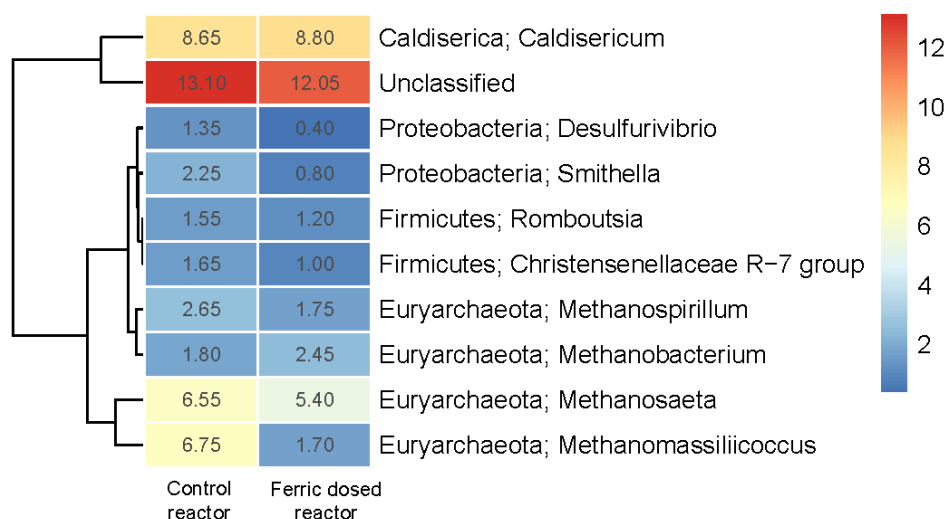
Figure S6. Heat map summarizing the percent relative abundances of bacteria (each row representing an OTU) in the biofilms collected from sewer biofilms. The relative similarity of each sample in terms of community composition as determined by complete linkage cluster analysis of OTU abundances is represented at the left of the heat map. Reads that could not be classified are collectively referred to as 'unclassified'.
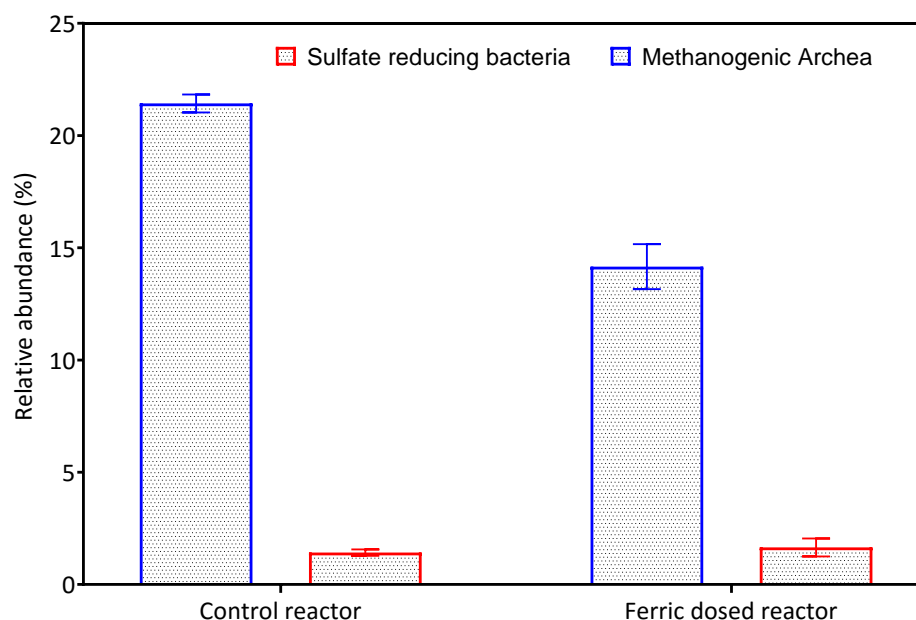

Figure S7. Relative abundance of SRB and MA in sewer biofilms.

S.4.2.2. ELEMENTAL COMPOSITION OF BIOFILM FROM THE FERRIC DOSED SEWER REACTOR

The EDS elemental mapping of the sewer biofilm obtained from the ferric dosed reactor has been shown in the Figure S8. The weight % shows that Fe and S are the two major fractions with 59.8% and 32.2% respectively. The atomic ratio of 1.06 was calculated based on this weight % suggesting the iron precipitate to be FeS in biofilms.
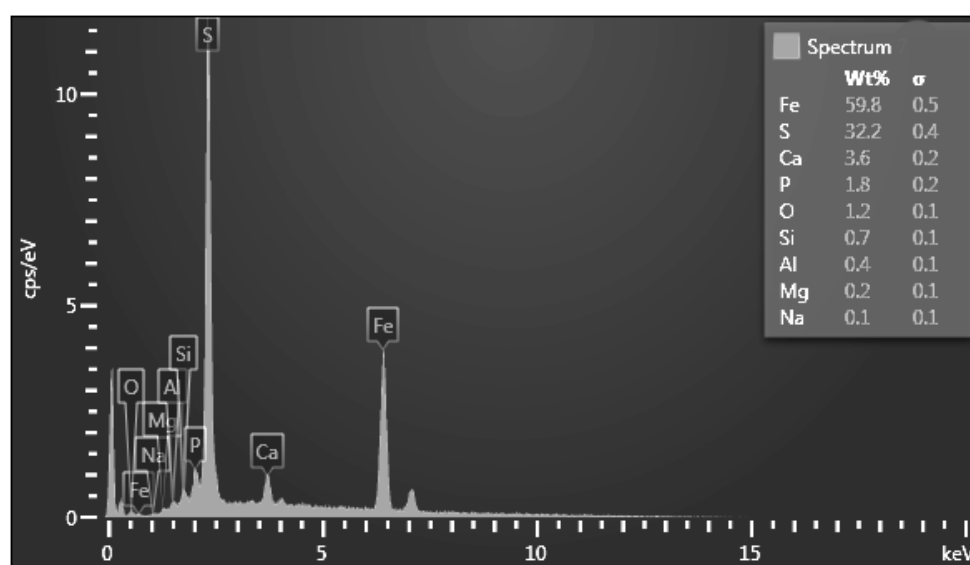

Figure S8. Elemental composition (wt %) of particles formed in the ferric dosed reactor by Energy Dispersive X-ray spectra

S.5. ADDITIONAL EXPERIMENTS TO INVESTIGATE THE ROLE OF VARIOUS IRON PARTICLES FORMED BY IRON DOSING

S.5.1. MATERIALS AND METHODS

S.5.1.1. BATCH TEST WITH SEWER REACTOR. The scope of this experiment is to investigate the removal of selected MPs by any other species of iron formed in the anaerobic sewer condition other than FeS. This experiment (6-hr) was conducted in the rising main sewer reactor to mimic the exact conditions described in section 2.4. But, in order to avoid the formation of FeS inside the reactor, all the wastewater in the reactor was drained to remove any pre-formed sulfides. Then, the experiment was carried out with fresh wastewater with no sulfide concentrations (<0.1 mg-S/L) in the wastewater. The wastewater was spiked with the selected MPs before feeding into the reactor. The background concentration of the spiked compounds was analysed to quantify the exact concentrations spiked. Fe^{3+} was added from a stock solution as described in section 2.3 to reach the theoretical concentration of 10 mg-Fe/L. The concentration of iron was chosen to replicate the experiment described in section 2.4. Wastewater samples were taken at a time interval of 1-hr throughout the cycle time of the reactor (6-hr) after the experiment started. For each time point, 2 mL of sample was filtered into a vial using 0.22 μm PES membrane syringe filter (Tullagreen, Ireland) and 20 μL of 2M HCl was added to adjust each of the samples to pH 2. The acidified samples were then frozen at −20°C until analysis.

S.5.1.2. BATCH TESTS WITH DIFFERENT FERRIC CONCENTRATIONS. Different iron precipitates, such as ferric oxide or hydroxides, can form at different dosages of ferric in wastewater. The scope of the batch tests is to investigate the impact of different concentration of iron (Fe^{3+}) (10, 5 and 1 mg-Fe/L) on the removal of selected MPs. The batch tests were conducted with filtered wastewater in serum bottles enclosed tightly with a rubber stopper to

maintain the anaerobic condition. The fresh wastewater with less sulfide concentration (<0.1 mg-S/L) was filtered using 5 micron water cartridge filter, to remove suspended solids. Selected MPs were then spiked in the filtered wastewater in the serum bottles. Mixing was continuously provided by a magnetic stirrer (Heidolph MR3000) at 250 rpm. The iron was dosed directly into the bottle and the bottles were covered with aluminum foil to avoid any potential photo-transformation process. The batch tests were carried out for 1-hr with the sampling interval of 30 min. Wastewater samples were taken as described in section 2.4 for the analysis of selected MPs.

S.5.2. RESULTS

S.5.2.1. BATCH TEST IN SEWER REACTOR. The batch results of iron dosing in the sewer reactor without pre-formed sulfide was compared with the results obtained in the control sewer reactors (section 2.4) without ferric dosing and is shown in the Figure S9. For the group-1 compounds, such as methadone, morphine and atenolol, no rapid removal was observed as obtained in the ferric dosed reactor (section 3.3.1). The ultimate removal of methadone, morphine and atenolol at the end of 6hr in this experiment reached up to 67.2%, 50.5% and 34.6% respectively. These results were similar to the results obtained in the control sewer reactor, suggesting negligible contribution of non-FeS iron precipitates in the removal of MPs. The ultimate removal of atenolol is comparatively lower in this experiment compared with the control sewer reactor. The possible explanation could be the reduced activity of microorganisms present in the biofilm during this experiment. Throughout the experiment the sulfate remained the same, explaining the reduced microbial activity of the biofilm. Similarly for morphine, the different profile observed could be due to reduced microbial activity inhibiting the back transformations of its glucuronides as discussed in section 3.3.1. The aforementioned results clearly emphasize that any other forms of iron precipitates were not

involved in the removal of these MPs. This supports our hypothesis that the suspended FeS formed in the anaerobic sewer reactors could be the reason for the observed rapid removal in the ferric dosed reactor (section 3.3.1). Similar to the Group-1 compounds, Group-2 & paracetamol showed the similar observations that the iron dosing in sewage without sulfides had no impact on their removal.
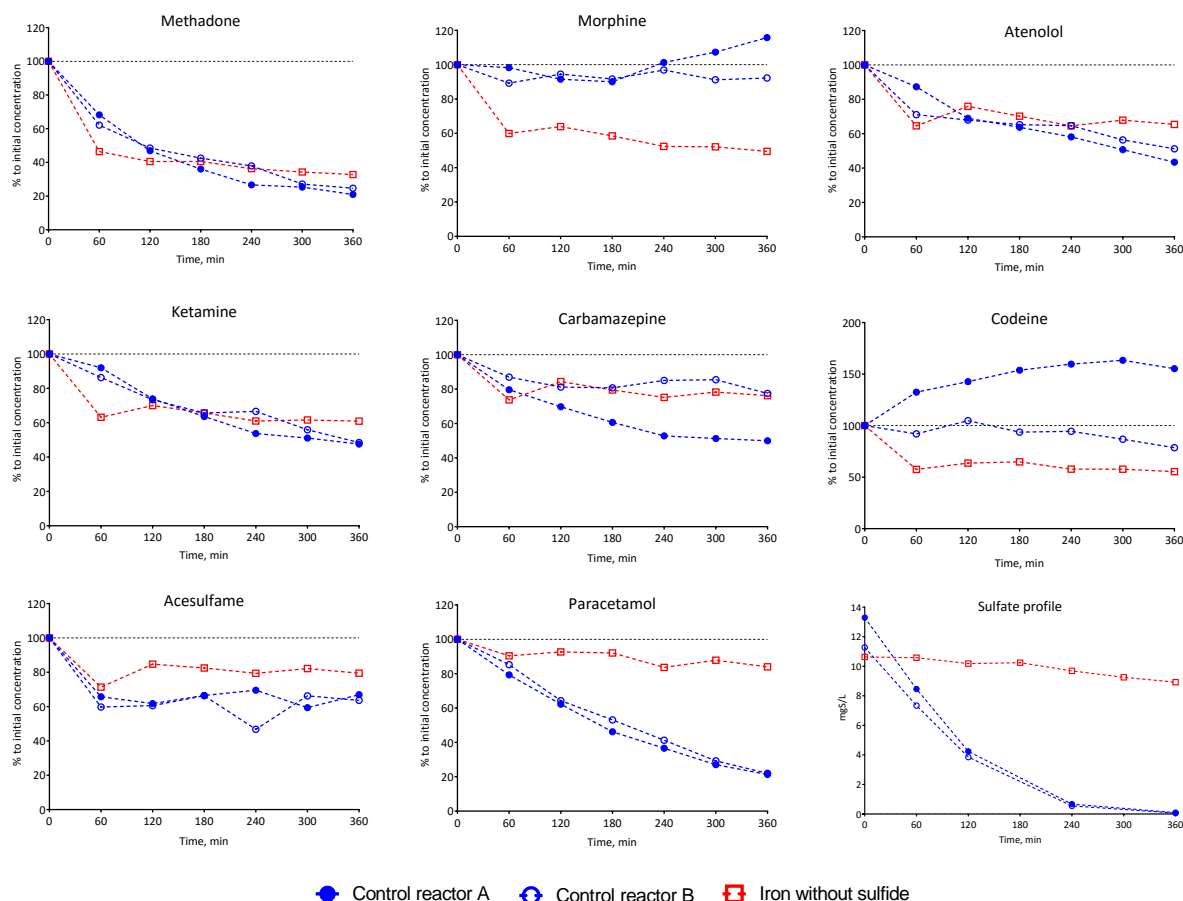

Figure S9. Removal of MPs due to Fe dosing in the non-sulfide anaerobic sewer reactor

S.5.2.2. BATCH TESTS WITH DIFFERENT FERRIC CONCENTRATIONS. The batch test with different Fe concentrations in the filtered wastewater is to further confirm the fate of different speciation of iron on the removal of selected MPs. The results were shown in the Figure S10. The different concentrations of ferric dosing (10, 5 and 1 mg-Fe/L) dosed showed

no impact on the MP concentrations as observed in section 3.5 (Figure S10). This indicates the

negligible effect of any other iron precipitates (such as ferric oxide or hydroxide) formed due

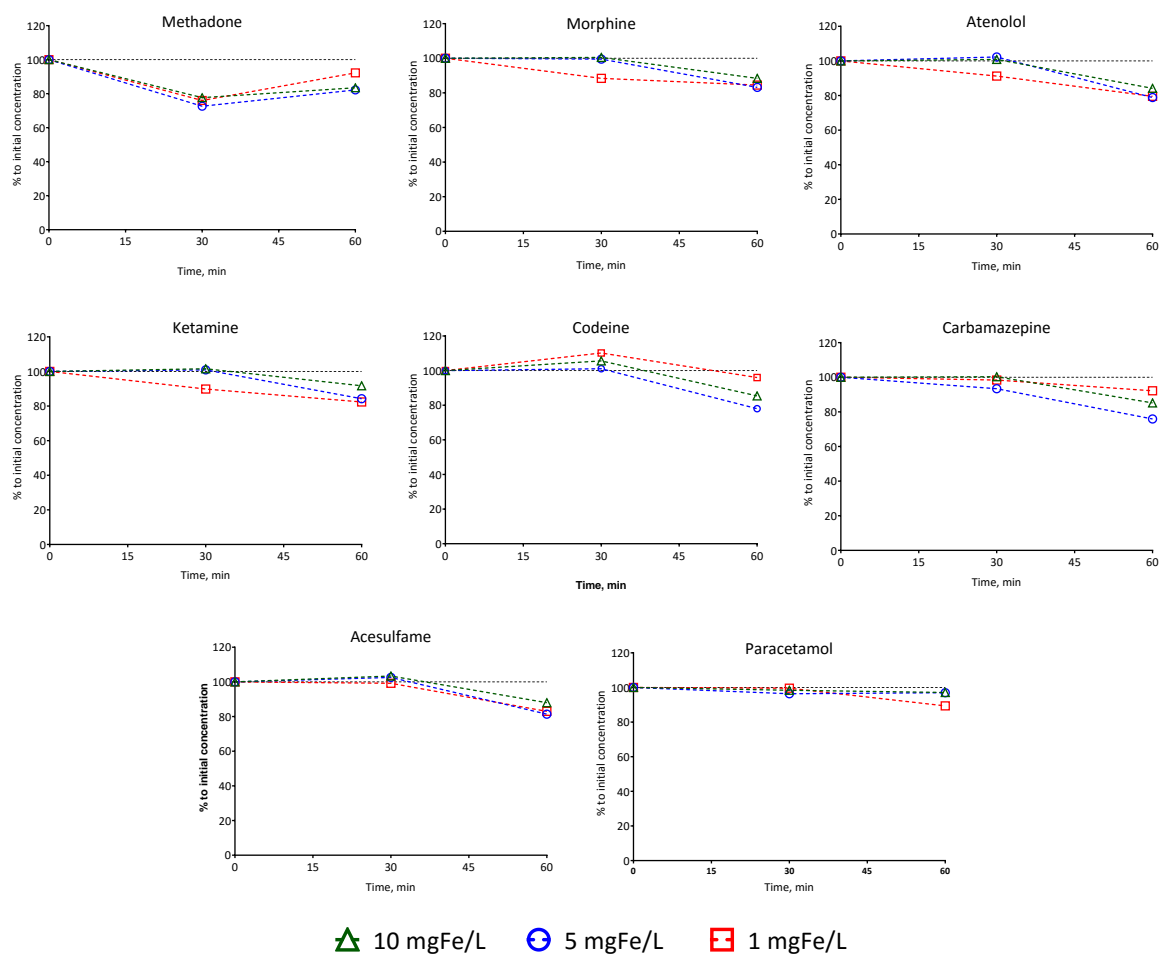to the hydrolysis on the removal of selected MPs.

Figure S10. Removal of MPs due to different Fe concentration in the filtered wastewater

REFERENCES

1.   Baker, D. R.; Kasprzyk-Hordern, B., Multi-residue determination of the sorption of illicit drugs and pharmaceuticals to wastewater suspended particulate matter using pressurised liquid extraction, solid phase extraction and liquid chromatography coupled with tandem mass spectrometry. *Journal of Chromatography A* **2011,** *1218*, (44), 7901-7913.

2.   van Nuijs, A. L. N.; Abdellati, K.; Bervoets, L.; Blust, R.; Jorens, P. G.; Neels, H.; Covaci, A., The stability of illicit drugs and metabolites in wastewater, an important issue for sewage epidemiology? *Journal of Hazardous Materials* **2012,** *239-240*, 19-23.

3.   Chen, C.; Kostakis, C.; Irvine Rodney, J.; Felgate Peter, D.; White Jason, M., Evaluation of pre-analysis loss of dependent drugs in wastewater: stability and binding assessments. *Drug Testing and Analysis* **2013,** *5*, (8), 716-721.

4.   Östman, M.; Fick, J.; Näsström, E.; Lindberg, R. H., A snapshot of illicit drug use in Sweden acquired through sewage water analysis. *Science of The Total Environment* **2014,** *472*, 862-871.

5.   Senta, I.; Krizman, I.; Ahel, M.; Terzic, S., Assessment of stability of drug biomarkers in municipal wastewater as a factor influencing the estimation of drug consumption using sewage epidemiology. *Science of The Total Environment* **2014,** *487*, 659-665.

6.   Ramin, P.; Libonati Brock, A.; Polesel, F.; Causanilles, A.; Emke, E.; de Voogt, P.; Plósz, B. G., Transformation and Sorption of Illicit Drug Biomarkers in Sewer Systems: Understanding the Role of Suspended Solids in Raw Wastewater. *Environmental Science & Technology* **2016,** *50*, (24), 13397-13408.

7.   McCall, A.-K.; Scheidegger, A.; Madry, M. M.; Steuer, A. E.; Weissbrodt, D. G.; Vanrolleghem, P. A.; Kraemer, T.; Morgenroth, E.; Ort, C., Influence of Different Sewer Biofilms on Transformation Rates of Drugs. *Environmental Science & Technology* **2016,** *50*, (24), 13351-13360.

8.   Gao, J.; Banks, A.; Li, J.; Jiang, G.; Lai, F. Y.; Mueller, J. F.; Thai, P. K., Evaluation of in-sewer transformation of selected illicit drugs and pharmaceutical biomarkers. *Science of The Total Environment* **2017,** *609*, 1172-1181.

9.   Lakshmanan, R.; Sanchez-Dominguez, M.; Matutes-Aquino, J. A.; Wennmalm, S.; Kuttuva Rajarao, G., Removal of Total Organic Carbon from Sewage Wastewater Using Poly(ethylenimine)-Functionalized Magnetic Nanoparticles. *Langmuir* **2014,** *30*, (4), 1036-1044.

10.   Coates, J., Interpretation of Infrared Spectra, A Practical Approach. In *Encyclopedia of Analytical Chemistry*, 2006.

11.   Lauterbach, L.; Wang, H.; Horch, M.; Gee, L. B.; Yoda, Y.; Tanaka, Y.; Zebger, I.; Lenz, O.; Cramer, S. P., Nuclear resonance vibrational spectroscopy reveals the FeS cluster composition and active site vibrational properties of an O2-tolerant NAD+-reducing [NiFe] hydrogenase. *Chemical Science* **2015,** *6*, (2), 1055-1060.

12.   Blázquez, G.; Martín-Lara, M. A.; Tenorio, G.; Calero, M., Batch biosorption of lead(II) from aqueous solutions by olive tree pruning waste: Equilibrium, kinetics and thermodynamic study. *Chemical Engineering Journal* **2011,** *168*, (1), 170-177.

13.   Kiran, I.; Akar, T.; Tunali, S., Biosorption of Pb(II) and Cu(II) from aqueous solutions by pretreated biomass of Neurospora crassa. *Process Biochemistry* **2005,** *40*, (11), 3550-3558.

14.   Cayford, B. I.; Dennis, P. G.; Keller, J.; Tyson, G. W.; Bond, P. L., High-throughput amplicon sequencing reveals distinct communities within a corroding concrete sewer system. *Applied and environmental microbiology* **2012,** *78*, (19), 7160-7162.

15.   Sobrieraj, M.; Boone, D., Smithella Liu, Balkwill, Aldrich, Drake and Boone 1999, 553 VP. *Bergey's Manual® of Systematic Bacteriology* **2005**, 1039-1040.

16.   Lee, J.; Kim, E.; Han, G.; Tongco, J. V.; Shin, S. G.; Hwang, S., Microbial communities underpinning mesophilic anaerobic digesters treating food wastewater or sewage sludge: A full-scale study. *Bioresource technology* **2018,** *259*, 388-397.

17.   Kahl, S.; Kleinsteuber, S.; Nivala, J.; van Afferden, M.; Reemtsma, T., Emerging Biodegradation of the Previously Persistent Artificial Sweetener Acesulfame in Biological Wastewater Treatment. *Environmental Science & Technology* **2018,** *52*, (5), 2717-2725.

18.   Maspolim, Y.; Zhou, Y.; Guo, C.; Xiao, K.; Ng, W. J., The effect of pH on solubilization of organic matter and microbial community structures in sludge fermentation. *Bioresource technology* **2015,** *190*, 289-298.

19.   Mori, K.; Yamaguchi, K.; Sakiyama, Y.; Urabe, T.; Suzuki, K.-i., Caldisericum exile gen. nov., sp. nov., an anaerobic, thermophilic, filamentous bacterium of a novel bacterial phylum, Caldiserica phyl. nov., originally called the candidate phylum OP5, and description of Caldisericaceae fam. nov., Caldisericales ord. nov. and Caldisericia classis nov. *International journal of systematic and evolutionary microbiology* **2009,** *59*, (11), 2894-2898.

20.   Kuribayashi, K.; Kobayashi, Y.; Yokoyama, K.; Fujii, K., Digested sludge-degrading and hydrogen-producing bacterial floras and their potential for biohydrogen production. *International Biodeterioration & Biodegradation* **2017,** *120*, 58-65.

21.   Jiao, J.; Wu, J.; Wang, M.; Zhou, C.; Zhong, R.; Tan, Z., Rhubarb supplementation promotes intestinal mucosal innate immune homeostasis through modulating intestinal epithelial microbiota in goat kids. *Journal of agricultural and food chemistry* **2018,** *66*, (4), 1047-1057.

22.   Lee, J.; Shin, S. G.; Han, G.; Koo, T.; Hwang, S., Bacteria and archaea communities in full-scale thermophilic and mesophilic anaerobic digesters treating food wastewater: Key process parameters and microbial indicators of process instability. *Bioresource technology* **2017,** *245*, 689-697.

23.   Satoh, H.; Odagiri, M.; Ito, T.; Okabe, S., Microbial community structures and in situ sulfate-reducing and sulfur-oxidizing activities in biofilms developed on mortar specimens in a corroded sewer system. *Water research* **2009,** *43*, (18), 4729-4739.

24.   Cypionka, H., Oxygen respiration by Desulfovibrio species. *Annual Reviews in Microbiology* **2000,** *54*, (1), 827-848.

25.   Kiilerich, B.; Brejnrod, A. D.; Vollertsen, J.; Kiilerich, P., Variations in microbiome composition of sewer biofilms due to ferrous and ferric iron dosing. *Cogent Environmental Science* **2019,** *5*, (1).

26.   Jin, P.; Shi, X.; Sun, G.; Yang, L.; Cai, Y.; Wang, X. C., Co-Variation between Distribution of Microbial Communities and Biological Metabolization of Organics in Urban Sewer Systems. *Environmental Science & Technology* **2018,** *52*, (3), 1270-1279.